QFT Based Gain-Scheduling Control Design for Linear Time-Varying Systems

Jae Weon Choi[1] and Ki Hong Im[2]
School of Mechanical Engineering and RIMT
Pusan National University, Pusan 609-735, KOREA

J. Jim Zhu[3]
Department of Electrical and Computer Engineering
Louisiana State University, Baton Rouge, LA 70803-6430, U.S.A.

Abstract

Most of linear time-varying(LTV) systems except special cases have no general solution for the dynamic equations. Thus, it is difficult to design time-varying controllers in analytic ways, and other control design approaches such as robust control and gain-scheduling have been applied to control design for the LTV systems. A robust control method such as quantitative feedback theory(QFT) has an advantage of guaranteeing the stability and the performance specification in frozen time sense. However, if these methods are applied to the approximated linear time-invariant(LTI) plants with large uncertainty, the designed control will be constructed in complicated forms and usually not suitable for fast dynamic performance. In this paper, as a method to enhance the fast dynamic performance, the approximated uncertainty of time-varying parameters are reduced by the proposed gain-scheduling control design based on QFT for LTV systems with bounded time-varying parameters. To generate a continuous and smooth gain-scheduling function, multi-layer neural network is used.

1 Introduction

To design controllers for LTV systems, robust control for uncertain LTI systems that are the approximation of LTV systems have been generally used because the analytic control design for LTV systems does not exist. However, these methods are not sufficient to reflect the fast dynamics of the original time-varying systems such as missiles and supersonic aircrafts because the approximated uncertainty region of time-varying parameters is too large. To solve this problem, the large uncertainty region is reduced by using finite number of LTI sub-models that have smaller uncertainties of each scheduling interval instead of largely time-varying model. Then, control parameter sets are constructed by using QFT design. QFT[1-3] is a frequency domain control design proposed by Isaac Horowitz. It is a design technique utilizing the Nichols chart(NC) to achieve a desired stability and performance tolerances over the specified region of plant parameter uncertainties[4]. As depicted in Figure 1, QFT control system uses 2DOF control design that includes a prefilter block $F(s)$ and a compensator block $G(s)$. QFT design transforms the specified parameter uncertainties into NC template and all the given specifications into NC bounds. Then, a control design that satisfies the specifications can be found by loop-shaping[5-7]. Because a general QFT design is used as it is, QFT design will not mentioned any more in this paper. The detailed contents about QFT can be found in several references, [3],[8],[9].

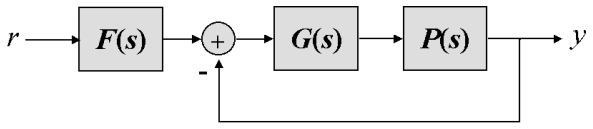

Figure 1: Block diagram of general QFT control system.

In this paper, to extend the performance and the stabilizing properties of QFT to the control design of LTV systems, QFT control parameter scheduling is performed. As the result, all the designed sub-systems will cover relatively small varying portion of time-varying parameters and the designed gain-scheduling control will guarantee the stability and the performance specifications in frozen time sense. The proposed design method is illustrated by a numerical example.

2 Gain-Scheduling Control Design Based on QFT for LTV Systems

2.1 Generalization of Scheduling Errors and Uncertainties

In this section, generalized scheduling error and corresponding uncertainty region evaluation of a bounded time-varying parameter is introduced. Using this re-

[1] Assistant professor,
[2] Graduate student,
[3] Associate professor.

sult, the number of LTI sub-models that are the approximation of time-varying model can be determined.

General time-varying systems considered as a nominal plant in this paper are of the form :

$$\begin{aligned} \dot{x}(t) &= A(t)x(t) + B(t)u(t) \\ y(t) &= C(t)x(t) + D(t)u(t) \end{aligned} \tag{1}$$

Assume that all the time-varying system parameters in *Eq.*(1) and the derivatives are continuous and bounded as

$$\begin{aligned} (a_{ij})_{\min} \le a_{ij}(t) \le (a_{ij})_{\max} \\ (b_{ij})_{\min} \le b_{ij}(t) \le (b_{ij})_{\max} \\ (c_{ij})_{\min} \le c_{ij}(t) \le (c_{ij})_{\max} \\ (d_{ij})_{\min} \le d_{ij}(t) \le (d_{ij})_{\max} \\ (\bar{a}_{ij})_{\min} \le \dot{a}_{ij}(t) \le (\bar{a}_{ij})_{\max} \\ (\bar{b}_{ij})_{\min} \le \dot{b}_{ij}(t) \le (\bar{b}_{ij})_{\max} \\ (\bar{c}_{ij})_{\min} \le \dot{c}_{ij}(t) \le (\bar{c}_{ij})_{\max} \\ (\bar{d}_{ij})_{\min} \le \dot{d}_{ij}(t) \le (\bar{d}_{ij})_{\max} \end{aligned} \tag{2}$$

where $a_{ij}(t), b_{ij}(t), c_{ij}(t)$, and $d_{ij}(t)$ are the time-varying elements of $A(t), B(t), C(t)$, and $D(t)$ respectively.

Since the values and the derivatives of parameters in general system that works properly in the real world must have values within the finite regions, *Eq.*(2) can be applied without loss of generality.

For instance, if an arbitrary time-varying parameter $v(t)$ depicted by a solid line in Figure 2 is given, it satisfies $v_{\min} \le v(t) \le v_{\max}, (\bar{v})_{\min} \le \dot{v}(t) \le (\bar{v})_{\max}$. Therefore LTV system parameters in *Eq.*(2) can be considered in the same way.

If the gain-scheduling interval is set as $T = 0.5$, nominal values of $v(t)$ in each scheduling interval can be determined as $v(t) \rightarrow v_k = v(k \times T)$ $(k = 1, 2, \cdots)$ and are depicted in Figure 2 with '$\times$'. For the first scheduling interval, $0.25 \le t < 0.75$, the upper and the lower scheduling errors of v_1 due to the time-varying property can be determined as positive values δv_{1u}, δv_{1l}, respectively. The dashed-circles r_k $(k = 1, 2, \cdots)$ in Figure 2 mean the sufficient range to contain the time-varying ranges of the kth scheduling interval. Figure 3 shows the detailed relation between the scheduling error and the radius of circle for kth interval.

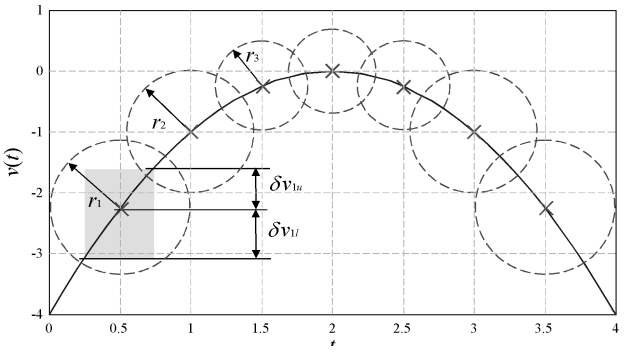

Figure 2: Scheduling errors of a time-varying parameter.

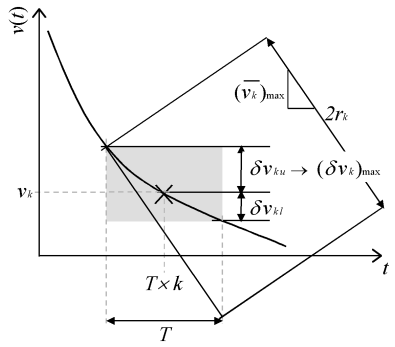

Figure 3: Radius of circle to contain the error bound.

From this relation, the maximum error $(\delta v_k)_{\max}$ and radius of the circle r_k of kth scheduling interval can be determined as

$$(\delta v_k)_{\max} = \max\left[\delta v_{ku}, \delta v_{kl}\right] \tag{3}$$

$$(\bar{v}_k)_{\max} = \max\left[|\dot{v}(t)|\right], ((k-0.5)T \le t < (k+0.5)T) \tag{4}$$

$$r_k = \frac{T}{2} \times (\bar{v}_k)_{\max} \tag{5}$$

The relation between $(\delta v_k)_{\max}$ and r_k can be represented as

$$r_k > (\delta v_k)_{\max} \tag{6}$$

As depicted in Figure 2, the values of $(\delta v_k)_{\max}$ and r_k are varying with time. Thus, for constructing design specifications that is independent of time, the generalization of $(\delta v_k)_{\max}$ and r_k are needed using the larger value than the maximum value of the entire time.

The real maximum scheduling error $(\delta v)_{\max}$ and the larger value E_v can be determined as *Eq.*(7) and *Eq.*(8) using maximum gradient of the parameter.

$$(\delta v)_{\max} = \max_k \left[(\delta v_k)_{\max}\right] \tag{7}$$

$$E_v = \frac{T}{2} \times \max\left[|(\bar{v})_{\min}|, |(\bar{v})_{\max}|\right] \tag{8}$$

$$(\delta v)_{\max} \le E_v \tag{9}$$

Because the maximum gradient is a fixed value, E_v can be used instead of $(\delta v)_{\max}$ as the generalized value of scheduling error $(\delta v_k)_{\max}$ regardless of time.

In the same manner, R_v, the generalized value of r_k, can be determined as

$$\begin{aligned} R_v &= \max_k \left[r_k\right] \\ &= \frac{T}{2}\left[1 + \left\{\max\left[|(\bar{v})_{\min}|, |(\bar{v})_{\max}|\right]\right\}^2\right]^{\frac{1}{2}} \end{aligned} \tag{10}$$

$$R_v > E_v \tag{11}$$

From *Eq.*(9) and *Eq.*(11), for any scheduling interval, E_v can be regarded as a maximum scheduling error and R_v as an uncertainty bound that sufficiently represents E_v in frozen time sense. Thus, the scheduling error and the uncertainty bound of any time-varying parameter can be determined by using *Eq.*(8) and *Eq.*(10), respectively.

2.2 LTV System Approximation Using Finite Number of LTI Sub-Models

In this section, the approximation of LTV system is performed by using finite number of LTI sub-models that have smaller uncertainties determined by the method of *Eq.*(10).

By applying to each scheduling interval, system matrix $A(t)$ in *Eq.*(1) can be represented as

$$A(t) \rightarrow A_k = A(k \times T) \quad (k = 1, 2, \cdots) \tag{12}$$

Other matrices $B(t), C(t)$, and $D(t)$ can be represented in the same manner.

Then, by taking the Laplace transformation, the system that have nominal parameter values of kth interval can be transformed into the transfer matrix

$$P_k(s) = C_k \left[sI - A_k\right]^{-1} B_k + D_k \tag{13}$$

For example, in case of SISO plant or an element of $P_k(s)$, a general nth order transfer function is as following form:

$$p_k(s) = \frac{(b_m)_k\, s^m + (b_{m-1})_k\, s^{m-1} + \cdots + (b_0)_k}{s^n + (a_{n-1})_k\, s^{n-1} + \cdots + (a_0)_k} \quad (m \leq n) \tag{14}$$

Since the frequency domain parameters in *Eq.*(14) such as $(a_{n-1})_k, \cdots, (a_o)_k$, $(b_m)_k, \cdots, (b_o)_k$ are determined by using the time domain parameters in A_k, B_k, C_k, and D_k, uncertainty bounds of both domain also have the same relation. Correspondingly, if the finite number of time domain LTI sub-models that have smaller uncertainties are able to cover the entire variation of original model, the sub-models are also able to cover the variation of the original model in the frequency domain.

In Figure 4, how to select finite number of LTI subsystems as the approximation of LTV system is presented. For example, a system that have two time-varying system parameters, $v_1(t)$ and $v_2(t)$, is considered. The parameter varying ranges of given LTV system is depicted by the area filled with gray color and

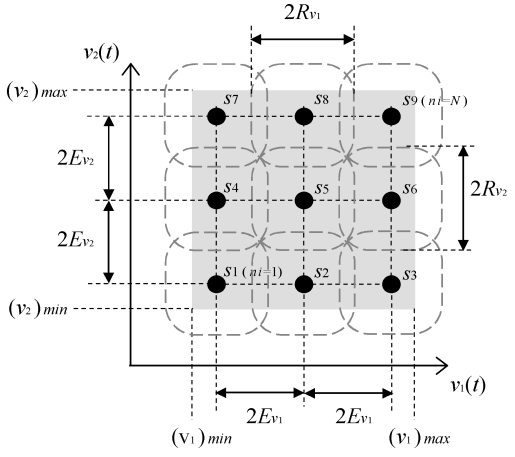

Figure 4: Selection of finite number of LTI sub-models.

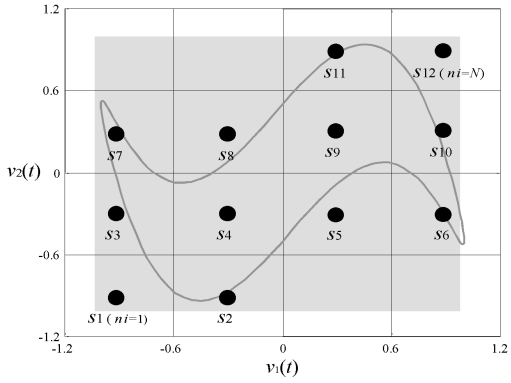

Figure 5: Selection of LTI sub-models for periodic LTV systems.

the selected LTI sub-systems, s_{ni} $(ni = 1, 2, \cdots, N)$, are depicted with '●'. Each dashed-box represents the uncertainty region that should be covered by subsystem located at the center. To determine the number and the parameter values of LTI sub-models, the parameter varying range is divided into smaller ranges using generalized scheduling errors, E_{v_1} and E_{v_2}, of the system parameters. Then the frozen time parameters of time-varying parameters located at the center of the smaller range will construct a sub-system depicted with '●'. In this manner, the largely varying parameter range of LTV system can be sufficiently covered by the finite number of sub-systems having smaller region of uncertainty in the frozen time sense. The number of the selected sub-systems is determined as

$$N = \prod_{p=1}^{q} \left[\text{int} \left(\frac{(v_p)_{\max} - (v_p)_{\min}}{2E_{v_p}} \right) + 1 \right] \tag{15}$$

where q denotes a total number of time-varying system parameter($q = 2$ in case of Figure 4), v_p denotes the pth time-varying parameter of the system, E_{v_p} denotes the generalized scheduling error of v_p, and $(v_p)_{\max(\min)}$ denotes the maximum(minimum) value of v_p.

Because the generalized scheduling error that is used in dividing parameter varying range and selecting submodels is a maximum value, the selected number N in *Eq.*(15) is a minimum value. Thus, the minimum number of LTI sub-models can be constructed for the approximation of LTV system.

For a special case, time-varying systems that have periodically varying parameters can be approximated with smaller number of sub-systems than that of general LTV systems. For example, the approximation of LTV systems with time-varying parameters, $v_1(t) = \sin(t)$ and $v_2(t) = \frac{\sin(3t)+\cos(t)}{2}$, is considered in Figure 5.

2.3 QFT Control Parameter-Scheduling by Using Neural Networks

The construction of QFT control parameter set of the selected LTI sub-models and gain-scheduling by an neural network are considered in this section.

An indispensable specification of QFT control design is the region of plant parameter uncertainty. As presented in previous sections, the generalized uncertainty such as R_v in *Eq.*(10) can be used as an parameter uncertainty of plants selected as LTI sub-models. Then, the uncertainty specification for the parameter $v(t)$ that should be covered by the nith selected sub-model can be represented as

$$-R_v \leq \Delta v_{ni} \leq R_v \ \ (ni = 1, \cdots, N) \tag{16}$$

where ni denotes selected sub-model number of Figure 4 and Figure 5.

The more general time-varying systems that have specified region of time-invariant parameter uncertainty are as following form:

$$\begin{aligned} \dot{x}(t) &= (A(t) + \Delta A)\, x(t) + (B(t) + \Delta B)\, u(t) \\ y(t) &= (C(t) + \Delta C)\, x(t) + (D(t) + \Delta D)\, u(t) \end{aligned} \tag{17}$$

$$\begin{aligned} (\Delta a_{ij})_{\min} \leq \Delta a_{ij} \leq (\Delta a_{ij})_{\max} \\ (\Delta b_{ij})_{\min} \leq \Delta b_{ij} \leq (\Delta b_{ij})_{\max} \\ (\Delta c_{ij})_{\min} \leq \Delta c_{ij} \leq (\Delta c_{ij})_{\max} \\ (\Delta d_{ij})_{\min} \leq \Delta d_{ij} \leq (\Delta d_{ij})_{\max} \end{aligned}$$

In this case, all the contents described in previous sections can be applied without changes by modifying the uncertainty specification of selected sub-models for QFT design. For the time-varying parameter $v(t)$ that have additional time-invariant uncertainty $(\Delta v)_{\min} \leq \Delta v \leq (\Delta v)_{\max}$, the uncertainty specification for QFT design can be modified as

$$-R_v + (\Delta v)_{\min} \leq \Delta v_{ni} \leq R_v + (\Delta v)_{\max} \quad (ni = 1, \cdots, N) \tag{18}$$

Pre-filter transfer matrices $F(s)_{ni}$ and compensator transfer matrices $G(s)_{ni}$ that are guaranteeing the frozen time stability and performance specifications can be constructed by QFT control design for the sub-models. In this paper, it is assumed that all the elements of $F(s)_{ni}$ and $G(s)_{ni}$ can be represented as proper rational transfer function that have fixed form such as *Eq.*(14) for all the sub-models($ni = 1, \cdots, N$). Design of the fixed form controller can be performed manually by using the MATLAB QFT Toolbox[6] and the MIMO QFT CAD[3]. The MIMO QFT CAD developed by Sating is good for general MIMO plants. Also, the automatic loop-shaping of QFT design can be performed by the methods[10],[11] based on evolutionary algorithms, convex optimization, and so on.

Then, QFT gain scheduling can be performed by a control parameter scheduling of the fixed form transfer functions. There are several scheduling methods such as simple switching algorithm, multi-dimensional curve fitting, and intelligent method. In this case, neural networks(NN) are adopted to reduce the effect of the non-smooth change of the control gain and get more smooth controlled performance by generating simple mapping of the control parameter relation and more smooth real-time scheduling[12].

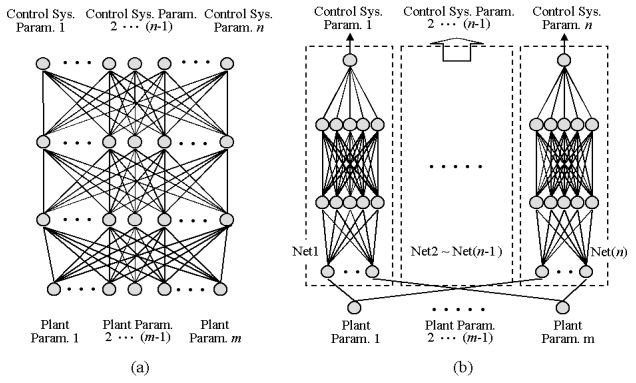

Figure 6: Neural network structures for control parameter mapping and scheduling.

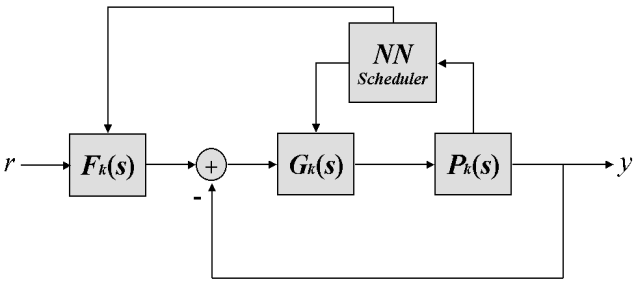

Figure 7: Block diagram of the whole control system.

The structure of the neural network used in this work is presented in Figure 6. Type (a) is a general form of multi-layer neural network. However, type (b) is more efficient for realizing fine mapping of control parameter, decoupling of parameter, and smaller number of connections that enables calculation time reduction. For mapping the control parameters into neural network by supervised learning, the selected nominal values of time-varying plant parameter sets of selected sub-models are used as input patterns and the designed control parameter sets as output patterns.

By using properly learned neural network as a control parameter scheduler, the whole QFT based gain-scheduling control system can be represented as Figure 7. Assuming the properly mapped relation of parameters, the continuous gain-scheduler enables us to apply the control system in Figure 7 to the reduced scheduling time interval. The available value of scheduling interval is represented as T_a in *Eq.*(19).

$$T_{NN} < T_a \leq T \tag{19}$$

where T_{NN} denotes the calculation time of neural network block and T is a scheduling time interval that is used in previous sections, respectively.

3 A Numerical Example

In this section, the proposed gain-scheduling control design is illustrated by a numerical example. The

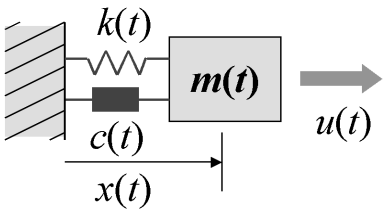

Figure 8: Time-varying MSD model.

plant for this example is the time-varying mass-spring-damper(MSD) model represented in Figure 8.

The dynamic equation of MSD model is as follows.

$$\begin{aligned}\ddot{x}(t) &= -\frac{k(t)}{m(t)}\,x(t) - \frac{c(t)+\dot{m}(t)}{m(t)}\,\dot{x}(t) + \frac{1}{m(t)}\,u(t) \\ &= -4x(t) - a(t)\dot{x}(t) + a(t)k(t)u(t) \end{aligned} \quad (20)$$

where the time-varying parameters, $a(t)$ and $k(t)$, are given as

$$\begin{aligned} a(t) &= 5\sin t + 8\,(3 \le a(t) \le 13) \\ k(t) &= 5\cos t + 8\,(3 \le k(t) \le 13) \end{aligned} \quad (21)$$

If the scheduling interval is set as $T = 0.4$, by *Eq.*(8) and *Eq.*(10), the generalized scheduling error and uncertainty can be determined as

$$\begin{aligned} E_a = E_k &= \frac{0.4}{2} \times 5 = 1 \\ R_a = R_k &= \frac{0.4}{2} \times \sqrt{1+5^2} \simeq 1 \end{aligned} \quad (22)$$

By using the generalized scheduling errors, E_a and E_k, the nominal point sets as $a_{ni} \in \{3,\ 5,\ 7,\ 9,\ 11,\ 13\}$ and $k_{ni} \in \{3,\ 5,\ 7,\ 9,\ 11,\ 13\}$ can be determined within the time-varying range of each parameter in *Eq.*(21). Since all the time-varying parameters given in this example are periodic functions, the number N of LTI sub-models can be determined as a smaller number than *Eq.*(15). Thus, by the generalized uncertainties R_a and R_k, the number of sub-models can be set as $N = 20$ and the parameter uncertainty specifications for QFT design of each sub-model can be determined as

$$\begin{aligned} -1 \le \Delta a_{ni} \le 1 \\ -1 \le \Delta k_{ni} \le 1 \quad (ni = 1, 2, \cdots, 20) \end{aligned} \quad (23)$$

And, for the performance specification, the maximum overshoot of unit step response is set to 1.1 for each of the sub-models.

The nith selected sub-model can be represented as

$$s_{ni}(s) = \frac{(k_{ni} + \Delta k_{ni})\,(a_{ni} + \Delta a_{ni})}{s^2 + (a_{ni} + \Delta a_{ni})\,s + 4} \quad (ni = 1, 2, \cdots, 20) \quad (24)$$

Then, the proper form of pre-filter and compensator transfer functions are fixed as

$$F_{ni}(s) = \frac{b_{F2}s^2 + b_{F1}s + b_{F0}}{s^3 + a_{F2}s^2 + a_{F1}s + a_{F0}} \quad (25)$$

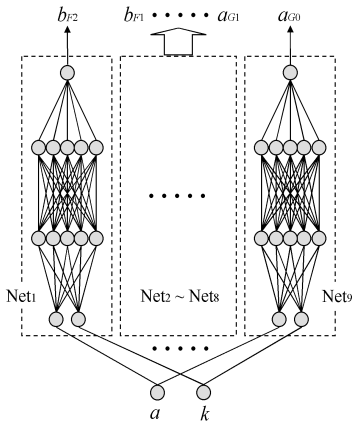

Figure 9: Neural network structure used in example.

$$G_{ni}(s) = \frac{b_{G1}s + b_{G0}}{s^2 + a_{G1}s + a_{G0}} \quad (26)$$

By using the transfer function forms presented above, QFT control design for each of the selected sub-models can be performed and the control parameter set for nith sub-model can be constructed as $\{\,a_{F0},\ a_{F1},\ a_{F2},\ b_{F0},\ b_{F1},\ b_{F2},\ \ a_{G0},\ a_{G1},\ b_{G0},\ b_{G1}\,\}_{ni}$ $(ni = 1, 2, \cdots, 20)$.

For the last step, the neural network as depicted in Figure 9 is constructed for control parameter-scheduling and perform the parameter relation mapping. The plant parameter set, a and k, of each sub-model is used as each input pattern and the designed QFT control parameter set in *Eq.*(25) and *Eq.*(26) is used as corresponding output pattern. In Figure 10, the mapping result of parameter relation between b_{F2} and the time-varying plant parameters is depicted.

The simulation of the numerical example is performed by applying the designed control system and the performance is compared with the existing QFT control in Figure 11 and Figure 12. The first simulation result, in case of the step input that have smaller time-varying property, shows that the two responses have similar tracking performance except the abnormal response of existing QFT control in $0 \le t \le 0.25$. However, in

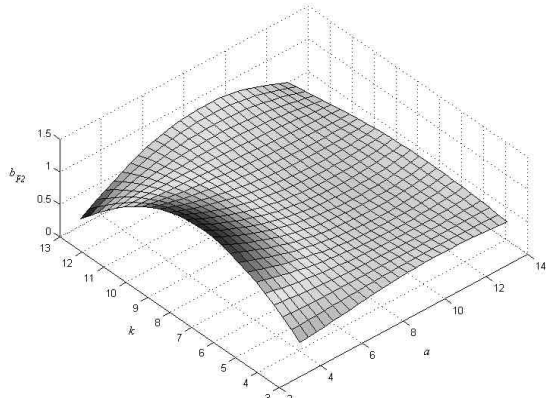

Figure 10: Mapping result of parameter b_{F2}.

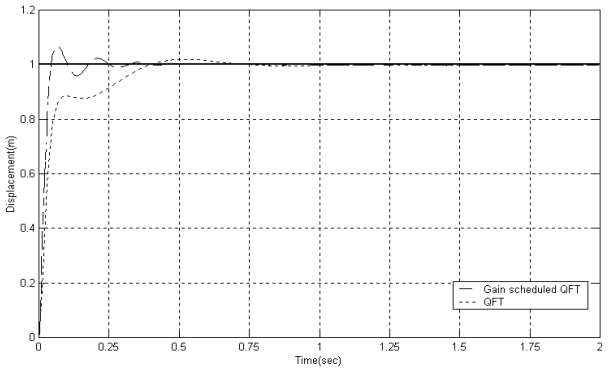

Figure 11: Step input response.

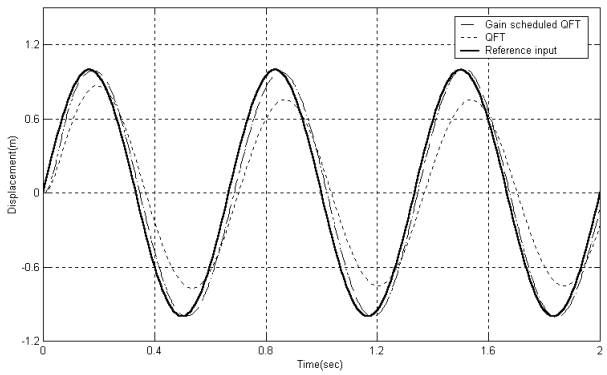

Figure 12: Sinusoidal input response.

case of a sinusoidal input that have larger time-varying property, the results shows more improved tracking performance of QFT gain-scheduling control than that of the existing QFT control.

4 Conclusions

In this paper, we proposed a gain-scheduling control design method based on QFT for LTV systems and the design procedures are illustrated by a numerical example. Further, the proposed method can be applied to LTV systems that have time-invariant parameter uncertainties, and the method guarantees the enhanced performance and the stability specification in frozen time sense. As confirmed by the simulation results, the QFT gain-scheduling control shows the more enhanced control performance in case of plants that have fast dynamics and highly time-varying command inputs. Thus, this control design will make more contributions to the control design of largely time-varying systems.

In this work, two points are considered as future works. One is an addition of on-line learning neural network because off-line learning neural network needs some trial and error for a performance guaranteeing parameter relation mapping with small number of pattern pairs. The other is the stability analysis of the whole control system including neural network using several methods such as an extension of stability for neural network control systems, hybrid system approaches, and so on.

References

[1] I. M. Horowitz, *Synthesis of feedback systems,* Academic Press, 1963.

[2] I. M. Horowitz, "Survey of quantitative feedback theory," *International Journal of Control*, vol. 53, no. 2, 1991, pp. 255-291.

[3] C. H. Houpis, R. R. Sating, S. Rasmussen, and S. Sheldon, "Quantitative feedback theory technique and applications," *International Journal of Control*, vol. 59, no. 1, 1994, pp. 39-70.

[4] Y. Chait, "Robust internal stability in multi input-output quantitative feedback theory," *Proceedings of the 30th Conference on Decision and Control*, 1991, pp. 2970-2971.

[5] C. F. Lin, *Advanced control systems design,* Prentice Hall, 1994.

[6] C. Borghesani,O. Yaniv, and Y. Chait, *Quantitative feedback theory toolbox user's guide,* The Mathworks, 1994.

[7] I. M. Horowitz, *Quantitative feedback theory(QFT),* QFT Publications, 1992.

[8] D. J. Leith, and W. E. Leithead, "Appropriate realization of MIMO gain-scheduled controllers," *International Journal of Control*, vol. 70, no. 1, 1998, pp. 13-50.

[9] D. J. Leith, and W. E. Leithead, "Gain-scheduled and nonlinear systems: dynamic analysis by velocity-based linearization families," *International Journal of Control*, vol. 70, no. 2, 1998, pp. 289-317.

[10] G. D. Halikias, and G. F. Bryant, "Optimal loop-shaping for systems with large parameter uncertainty via linear programming," *International Journal of Control*, vol. 62, no. 1, 1995, pp. 557-568.

[11] W. H. Chen, D. J. Ballance, W. Feng, and Y. Li, "Genetic algorithm enabled computer-automated design of QFT control systems," *Proceedings of the 1999 IEEE International Symposium on Computer Aided Control System Design*, 1999, pp. 492-497.

[12] H. Demuth, and M. Beale, *Neural network toolbox user's guide,* The Mathworks, 1997.